



Libraries and Learning Services

University of Auckland Research Repository, ResearchSpace

Version

This is the publisher's version. This version is defined in the NISO recommended practice RP-8-2008 <http://www.niso.org/publications/rp/>

Suggested Reference

Wang, Z., & Grimson, M. (2016). Dynamic response in a finite size composite multiferroic thin film. *Journal of Applied Physics*, 119(12), 124105.
doi: [10.1063/1.4944604](https://doi.org/10.1063/1.4944604)

Copyright

Items in ResearchSpace are protected by copyright, with all rights reserved, unless otherwise indicated. Previously published items are made available in accordance with the copyright policy of the publisher.

For more information, see [General copyright](#), [Publisher copyright](#), [SHERPA/RoMEO](#).

Dynamic response in a finite size composite multiferroic thin film

Zidong Wang and Malcolm J. Grimsom

Citation: *Journal of Applied Physics* **119**, 124105 (2016); doi: 10.1063/1.4944604

View online: <http://dx.doi.org/10.1063/1.4944604>

View Table of Contents: <http://scitation.aip.org/content/aip/journal/jap/119/12?ver=pdfcov>

Published by the [AIP Publishing](#)

Articles you may be interested in

[Low moment NiCr radio frequency magnetic films for multiferroic heterostructures with strong magnetoelectric coupling](#)

J. Appl. Phys. **111**, 103915 (2012); 10.1063/1.4722344

[Residual stress and magnetic behavior of multiferroic \$\text{CoFe}_2\text{O}_4/\text{Pb}\(\text{Zr}_{0.52}\text{Ti}_{0.48}\)\text{O}_3\$ thin films](#)

J. Appl. Phys. **105**, 084113 (2009); 10.1063/1.3115452

[Influence of relative thickness on multiferroic properties of bilayered \$\text{Pb}\(\text{Zr}_{0.52}\text{Ti}_{0.48}\)\text{O}_3 - \text{CoFe}_2\text{O}_4\$ thin films](#)

J. Appl. Phys. **104**, 114114 (2008); 10.1063/1.3035851

[Multiferroic nanoparticulate \$\text{Bi}_{3.15}\text{Nd}_{0.85}\text{Ti}_3\text{O}_{12} - \text{CoFe}_2\text{O}_4\$ composite thin films prepared by a chemical solution deposition technique](#)

Appl. Phys. Lett. **90**, 152903 (2007); 10.1063/1.2709946

[Multiferroic properties of \$\text{Pb}\(\text{Zr}, \text{Ti}\)\text{O}_3/\text{CoFe}_2\text{O}_4\$ composite thin films](#)

J. Appl. Phys. **100**, 126105 (2006); 10.1063/1.2400795

The advertisement features a blue background with a glowing light effect on the right. On the left, there is a small image of the journal cover for 'Applied Physics Reviews', which shows a diagram of a layered structure. The main text 'NEW Special Topic Sections' is in large, white, bold letters. Below this, the text 'NOW ONLINE' is in yellow, followed by 'Lithium Niobate Properties and Applications: Reviews of Emerging Trends' in white. The AIP Applied Physics Reviews logo is in the bottom right corner.

NEW Special Topic Sections

NOW ONLINE
Lithium Niobate Properties and Applications:
Reviews of Emerging Trends

AIP Applied Physics
Reviews

Dynamic response in a finite size composite multiferroic thin film

Zidong Wang (王子东),^{a)} and Malcolm J. Grimson

Department of Physics, The University of Auckland, Auckland 1010, New Zealand

(Received 26 November 2015; accepted 8 March 2016; published online 23 March 2016)

Composite multiferroics, heterostructures of ferromagnetic and ferroelectric materials, are characterized by a remarkable magnetoelectric effect at the interface. Previous work has supported the ferromagnetic structure with magnetic spins and the ferroelectric with pseudospins which act as electric dipoles in a microscopic model, coupled with a magnetoelectric interaction [Wang and Grimson, *J. Appl. Phys.* **118**, 124109 (2015)]. In this work, by solving the stochastic Landau-Lifshitz-Gilbert equation, the electric-field-induced magnetization switching in a twisted boundary condition has been studied, and a behavior of domain wall in the ferromagnetic structure is discussed. © 2016 AIP Publishing LLC. [<http://dx.doi.org/10.1063/1.4944604>]

I. INTRODUCTION

A. Composite multiferroic materials

Recently, the discovery of coupled ferromagnetism and ferroelectricity has strongly revived interest in the field of multiferroism, theoretically^{1–6} and experimentally,^{7,8} due to the remarkable effects of the induced magnetization by applying an electric field and the induced polarization by an applied magnetic field.⁹ This phenomenon is called magnetoelectric effect. Curie first discovered this effect in 1894,¹⁰ and it was experimentally confirmed by Astrov in 1960.¹¹ So far, the mechanism that causes the emergence of the magnetoelectric effect in the ferromagnetic (FM)/ferroelectric (FE) coupled multiferroics is still under discussion. One common origin is the strain-stress coupling.^{12,13} Generally, FE materials display the behaviors of piezoelectricity and electrostriction. This provides, respectively, linear and quadratic shape deformations to an applied field. Similarly, FM materials display piezomagnetism and magnetostriction which can lead an external stress induced magnetic response. Thus, the combination of FM and FE phases generates an enormous magnetoelectric effect.^{14,15} Electrostatic screening provides another origin, and this has been studied by Jia *et al.*¹⁶ In this paper, we consider a general linear and quadratic magnetoelectric couplings at the FM/FE interface.

B. Spin and pseudospin models

Previous works have discussed a numerical modeling for field-driven composite multiferroics by the spin dynamics approach.^{1,3,17} Generally, the technique of the spin dynamics is used to solve the behavior of the magnetic moment due to an effective field in the micromagnetic model.¹⁸ In this model, the magnetic moment is replaced by the spin moment in each individual magnetic spin. The classic Heisenberg model can be used to describe the total free energy stored in this system.¹⁹ FE materials normally contain electric dipoles. In the framework of spin dynamics, the electric dipoles are represented by the pseudospins, with a transverse Ising model to characterize the local energy.²⁰ The transverse

Ising model was conjectured by de Gennes²¹ and Elliott,²² for the description of order-disorder KDP-type ferroelectrics (e.g., KH_2PO_4 and NaNO_2). Later, the transverse Ising model was also used for displacive type ferroelectrics (e.g., BaTiO_3 and PbTiO_3).²³ The novelty here is that we have developed a variable-size pseudospin to compare with the electric dipole in the dielectric materials.²⁴ A variable-size pseudospin can change its length when an enormous electric field applied, as the separation of an electric dipole.

C. Article outline

The aim of present work is to demonstrate the magnetization switching behavior, due to electric field induced polarization with a twisted boundary condition.²⁵ The numerical result shows the control of the magnetic domain wall structure in the FM lattice.²⁶ The technical details of the model and the simulation method are introduced in Section II. In Section III, the results are revealed and discussed. Section IV is devoted to the summary and perspectives for future application.

II. MODEL AND METHOD

A. Composite multiferroic thin film

In the spirit of a coarse-graining approach, the FM/FE coupled thin film has been considered by a two dimensional heterostructure lattice, with a finite size of L layers in each side and N elements in each layer. The schematic view is in Fig. 1, with the magnetic spins (red arrows) and the electric pseudospins (blue arrows). This lattice is glued by the magnetoelectric coupling at the interface (yellow line) between the last FM layer and the first FE layer. Note that the FM lattice uses twisted boundaries (black arrows) on left- and right-hand sides, in order to show the behavior of the domain wall shifting. The other edges use open (free) boundary condition.

The total energy for the microscopic model can be written as a sum of three main terms in Eq. (1). The first two terms describe the local energies stored in the FM and FE lattices, respectively, and the third term describes the magnetoelectric interaction between the FM and the FE structures.

^{a)}E-mail: Zidong.Wang@auckland.ac.nz

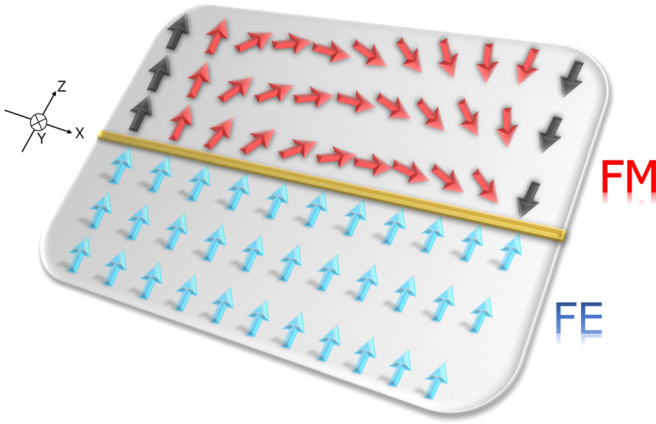


FIG. 1. Schematic illustration of the magnetic spins (red) and the electric pseudospins (blue) in the FM/FE coupled lattice, with magnetolectric coupling at the interface (yellow). The FM structure with twisted boundaries (black).

$$\mathcal{H} = \mathcal{H}_{FM} + \mathcal{H}_{FE} + \mathcal{H}_{ME}. \quad (1)$$

B. Energy and dynamics in the FM lattice

In this study, the FM/FE coupled thin film has been regarded as a lattice model. In the FM lattice, the magnetic spin $S_{i,j} = (S_{i,j}^x, S_{i,j}^y, S_{i,j}^z)$ is a normalized operator with unit length, i.e., $\|S_{i,j}\| = 1$, $i, j \in [1, 2, 3, \dots, N]$ represents the location of each spin. The Hamiltonian of the magnetic subsystem \mathcal{H}_{FM} is modelled by the classical Heisenberg model, as

$$\mathcal{H}_{FM} = -J_{FM} \sum_{i,j} [S_{i,j} \cdot (S_{i+1,j} + S_{i,j+1})] - K_{FM}^z \sum_{i,j} (S_{i,j}^z)^2, \quad (2)$$

where the first term represents the nearest-neighbor exchange interaction, and $J_{FM}^* = J_{FM}/k_B T$ is the dimensionless exchange coefficient. The second term represents the uniaxial anisotropy, and $K_{FM}^* = K_{FM}^z/k_B T$ is the dimensionless uniaxial anisotropic coefficient in the z -direction.

To describe the time evolution of the spins' response, an differential equation named Landau-Lifshitz-Gilbert equation has been used at atomic level.^{1,18,27} In Eq. (3), the Landau-Lifshitz-Gilbert equation predicts the rotation of the magnetization in response to torques. See supplementary Movie 1 in in Ref. 28.

$$\frac{\partial S_{i,j}}{\partial t} = -\gamma_{FM} [S_{i,j} \times \mathbf{H}_{S_{i,j}}^{eff}] - \lambda_{FM} [S_{i,j} \times (S_{i,j} \times \mathbf{H}_{S_{i,j}}^{eff})], \quad (3)$$

where the gyromagnetic ratio γ_{FM} relates the magnetic spin to its angular momentum. λ_{FM} denotes the phenomenological Gilbert damping terms in the FM structures. The magnetic effective field $\mathbf{H}_{S_{i,j}}^{eff}$ in Eq. (3) is the derivative of the system Hamiltonian of Eq. (2) with respect to the magnitudes of the magnetic spin in each direction, as

$$\mathbf{H}_{S_{i,j}}^{eff} = -\frac{\delta \mathcal{H}_{FM}}{\delta S_{i,j}} = \left\{ \begin{array}{l} J_{FM} (S_{i+1,j}^x + S_{i,j+1}^x) + H_{S_{i,j}^x}^{stoch} \\ J_{FM} (S_{i+1,j}^y + S_{i,j+1}^y) + H_{S_{i,j}^y}^{stoch} \\ J_{FM} (S_{i+1,j}^z + S_{i,j+1}^z) + 2K_{FM}^z S_{i,j}^z + H_{S_{i,j}^z}^{stoch} \end{array} \right\}, \quad (4)$$

where $H_{S_{i,j}^{x,y,z}}^{stoch}$ characterizes a stochastic field on the x -, y -, and z -components, individually.

C. Energy and dynamics in the FE thin film

In order to deliver the electric dipole moment into the spin system, here we follow Elliott and Young,²² use a pseudospin model with the electric pseudospin $P_{i,j} = (P_{i,j}^x, P_{i,j}^y, P_{i,j}^z)$. $i, j \in [1, 2, 3, \dots, N]$ represent the location of each pseudospin. The Hamiltonian of the pseudospins is depicted by the transverse Ising model \mathcal{H}_{FE} is defined in Eq. (5) with local and external energies

$$\mathcal{H}_{FE} = -J_{FE} \sum_{i,j} [P_{i,j}^z (P_{i+1,j}^z + P_{i,j+1}^z)] - \Omega_{FE}^x \sum_{i,j} P_{i,j}^x - E_{ext}^z(t) \sum_{i,j} P_{i,j}^z, \quad (5)$$

where $J_{FE}^* = J_{FE}/k_B T$ is the dimensionless nearest-neighbor exchange interaction couplings between electric pseudospins. The second term stands for the transverse energy, where Ω_{FE}^x is the transverse field along the local x -axis, which is perpendicular to the Ising z -direction in the FE structure.^{29,30} The third term is the external energy caused by an applied time-dependent electric field $E_{ext}^*(t) = \epsilon_0 \chi_e E_{ext}^z(t)/k_B T$ in the z -direction, where ϵ_0 is the electric permittivity of free space, and χ_e is the susceptibility. Generally, the polarization P is proportional to the external electric field E_{ext} in the dielectric materials³¹

$$P = \epsilon_0 \chi_e E_{ext}. \quad (6)$$

Here, the size of the electric pseudospin is varied with its effective field $\mathbf{H}_{P_{i,j}}^{eff}$ (see Eq. (9) and Ref. 24)

$$\|P_{i,j}\| = \epsilon_0 \aleph_e \|\mathbf{H}_{P_{i,j}}^{eff}\|, \quad (7)$$

where \aleph_e is the dimensionless pseudoscalar susceptibility.

To solve the time evolution of the electric response in the FE structure, we use a spin dynamic method. The limitation of this technique is that the electric dipole moment, which is a measurement of the z -component separation of positive and negative charges, is a scalar. Thus, the time evolution of the pseudospins in the FE lattice are expected to perform a precession free trajectory^{1,3,24} following

$$\frac{\partial P_{i,j}}{\partial t} = -\lambda_{FE} [P_{i,j} \times (P_{i,j} \times \mathbf{H}_{P_{i,j}}^{eff})], \quad (8)$$

where λ_{FE} denote the phenomenological Gilbert damping terms in the FE lattice. This is shown in supplementary Movie 2 in Ref. 28. The magnitude of the z -component $P_{i,j}^z$ represents the electric polarization, and $P_{i,j}^x$ and $P_{i,j}^y$ are the pseudoscalar polarizations. The electric effective field $\mathbf{H}_{P_{i,j}}^{eff}$ in Eq. (8) for the pseudospin is defined as a functional derivative of Eq. (5)

$$\mathbf{H}_{P_{i,j}}^{eff} = -\frac{\delta \mathcal{H}_{FE}}{\delta P_{i,j}} = \left\{ \begin{array}{l} \Omega_{FE}^x \\ 0 \\ J_{FE} (P_{i+1,j}^z + P_{i,j+1}^z) + E^z(t) + H_{P_{i,j}^z}^{stoch} \end{array} \right\}, \quad (9)$$

where $H_{P_{ij}^z}^{stoch}$ characterizes the stochastic field. Note that x - and y -components are the pseudo-components of the pseudospin model and there is no thermal agitation.

D. Thermal effect

Thermal effect cannot be neglected. The orientation of the magnetic/electric moments is continuously changed by thermal agitation. We study a simplified Brownian motion by reducing the random forces to a purely random process.¹ This random process is added into the effective field of each magnetic spin or electric pseudospin as a stochastic field H^{stoch} , which is a white Gaussian noise, into the dynamics.³² The probability density function of this stochastic field is given as

$$\text{Pr} = \frac{1}{\sigma\sqrt{2\pi}} \exp\left[-\frac{(H^{stoch} - \mu)^2}{2\sigma^2}\right], \quad (10)$$

where μ is the mean and σ is the standard deviation of the Gaussian distribution. Since the existence of both the magnetization and the electric polarization is required at low temperatures, the standard deviation has been limited to $\sigma = 0.01$, without any bias (i.e., $\mu = 0$). Therefore, both Eqs. (3) and (8) become stochastic Landau-Lifshitz-Gilbert equations.

E. Magnetoelectric interactions

The last term in Eq. (1) characterizes the interfacial energy between the last FM layer and the first FE layer, which is described by the dipole-spin interaction Hamiltonian \mathcal{H}_{ME} with the magnetoelectric susceptibility g_m ,^{9,33} as

$$\mathcal{H}_{ME} = - \sum_m \sum_j g_m (S_{N,j}^z P_{1,j}^z)^m. \quad (11)$$

In this work, we only need to account for the low-energy excitations (i.e., piezoelectric/piezomagnetic effects and magnetostrictive/electrostrictive effects) at the interface and so restrict ourselves to the linear g_1 and quadratic g_2 terms only. Higher order terms have not been studied here, due to their minor relevant effects in the numerical modelling. Thus, the interfacial Hamiltonian used in the numerical simulations is

$$\mathcal{H}_{ME} = - \sum_j [g_1 (S_{N,j}^z P_{1,j}^z) + g_2 (S_{N,j}^z P_{1,j}^z)^2]. \quad (12)$$

III. RESULTS AND DISCUSSION

We implement a numerical simulation for the electric-field-driven multiferroic 16×16 square lattice sample, and a dimensionless parameter set $\{J_{FM}^* = J_{FE}^* = 1, K_{FM}^* = 0.1, \Omega_{FE}^* = 0.1, g_1^* = g_2^* = 1, \gamma_{FM}^* = 1, \text{ and } \lambda_{FM}^* = \lambda_{FE}^* = 0.1\}$, with twisted boundary conditions in the FM structure, and free boundary conditions for the rest. A rectangular electric field is applied in the local z -axis, with a dimensionless magnitude of $E_0^* = 10$. The simulation proceeds by a fourth order Runge-Kutta method.

The magnetization switching due to electric field induced polarization is shown in Fig. 2. In this figure, the

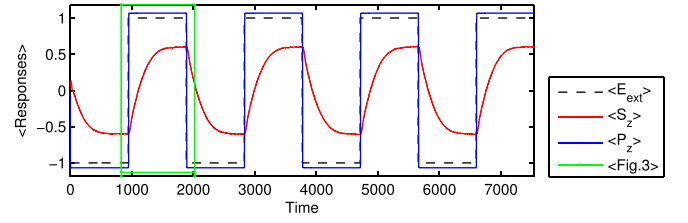


FIG. 2. The dynamic mean z -component magnitudes of the magnetic spins (red) and electric pseudospins (blue) are driven by a normalized rectangular electric field (black dashed).

dynamical progress of the mean magnetization $\langle S_z \rangle$ (red curve) and the mean polarization $\langle P_z \rangle$ (blue curve), i.e., the average magnitudes of the z -component in spins and pseudospins, to the normalized driven field $\langle E_{ext} \rangle$ (black dashed-curve). The electric polarization responds to flip over the direction immediately, due to its direct coupling to the electric field. The magnetization then catches up, the switching energy being transferred across the interface from the electric pseudospins by the magnetoelectric effect. The size of the electric pseudospins is limited by the pseudoscalar susceptibility \aleph_e . We find $\aleph_e = [(E_{ext}^z(t))^2 + (\Omega_{FE}^x)^2]^{-1}$ is the most appropriate for the size of electric pseudospin with the unit size of magnetic spin. Hence, in Fig. 2, the mean polarization of the electric pseudospin is in the linear dependence region.

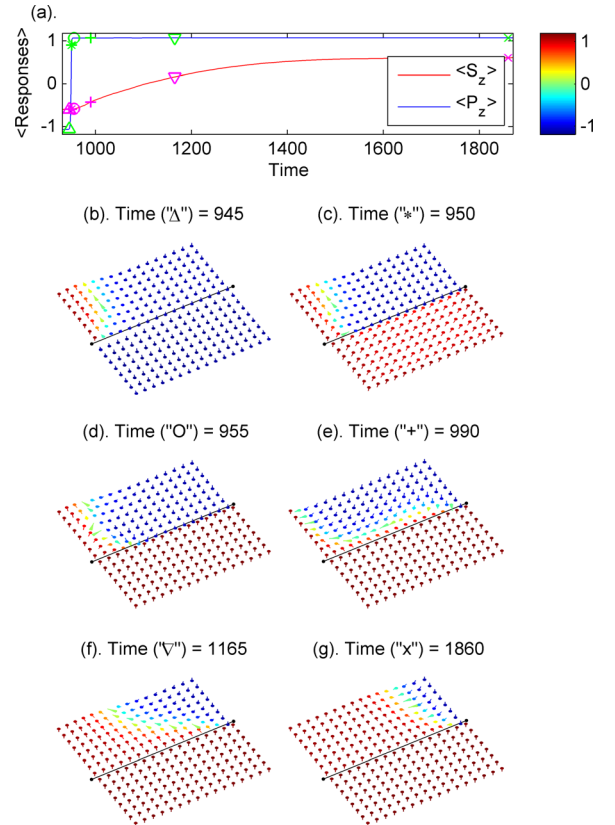


FIG. 3. (a) A closer inspection from Fig. 2 in a distinct region. (b)–(g) Six snapshots (symbols “ Δ ,” “ $*$,” “ O ,” “ $+$,” “ ∇ ,” and “ x ” in panel (a)) represent the phase states of the magnetic spins and electric pseudospins in the FM/FE coupled lattice at each particle time. The electric pseudospins are at front of the black line, and behind of the black line are the magnetic spins. The color scale represents the magnitude of the z -component. See supplementary Movies 3 and 4 in Ref. 28.

In order to observe finer detail, we take a distinct region, dimensionless time $t^* \in [900, 1900]$ shown by the green box in Fig. 2, and study the behavior of the domain wall in the driven part in Fig. 3. The six snapshots show the instantaneous states of the magnetic spins and electric pseudospins in the lattice in Figs. 3(b)–3(g). Their relevant time locations are shown in Fig. 3(a) with pink and green symbols, such as “ Δ ,” “*,” “O,” “+,” “ ∇ ,” and “X.” The multiple colors in Figs. 3(b)–3(g) characterize the magnitudes of the spins and pseudospins in the local z -direction. The black line at the middle in each panel represents the interface that divides the FE (front) and FM (behind) structures. In Fig. 3(b), the sequence starts from $t^*(\Delta) = 945$. At $t^*(*) = 950$, Fig. 3(c) shows the electric pseudospins reorienting. A short time later, $t^*(O) = 955$ in Fig. 3(d), the magnetic spins start reorientation close to the interfacial layer. At $t^*(+) = 990$, Fig. 3(e), the magnetic spins in the interfacial layer have flipped over and domain wall motion begins to diffuse to the further layers. The domain wall changes its shape when it shifts rightward. Because of the different speeds of the wall propagation in each layer in the FM structure. At $t^*(\nabla) = 1165$ in Fig. 3(f), the domain wall shows a more linear-like shape away from the interface. Much later, $t^*(X) = 1860$ in Fig. 3(g), the whole domain wall has attained an equilibrium state in the constant driving field that is determined by the twisted boundary condition.

IV. CONCLUSIONS

The spin dynamics approach allows us to solve the field-driven multiferroic system in a microscopic model. In this paper, the magnetic spin and electric pseudospin have been defined in a two dimensional lattice. We proposed them to investigate the electric-driven-magnetization switching property. In particular, using the twisted boundary condition, the behavior of the magnetic domain wall can be extracted. This analysis can facilitate designing composite multiferroic materials for relevant technological purposes, such as the control of the shifting of the magnetic domain wall via electric field can be applied to develop low-energy consuming electronic devices. Also, the manipulation of the electric properties by an external magnetic field also can be observed in this model.

ACKNOWLEDGEMENTS

Wang Zidong gratefully acknowledges Wang Feng (王峰) and Zhao Wen Xia (赵雯霞) for financial support.

- ¹Z. D. Wang and M. J. Grimson, *J. Appl. Phys.* **118**, 124109 (2015).
- ²Z. D. Wang and M. J. Grimson, *Eur. Phys. J.: Appl. Phys.* **70**, 30303 (2015).
- ³Z. D. Wang and M. J. Grimson, in 39th Annual Condensed Matter and Materials Meeting, Wagga Wagga, Australia, 3–6 February, 2015, <http://www.aip.org.au/info/?q=content/39th-annual-condensed-matter-and-materials-meeting>.
- ⁴A. Sukhov, C. L. Jia, P. P. Horley, and J. Berakdar, *J. Phys.: Condens. Matter* **22**, 352201 (2010).
- ⁵L. Chotorlishvili, R. Khomeriki, A. Sukhov, S. Ruffo, and J. Berakdar, *Phys. Rev. Lett.* **111**, 117202 (2013).
- ⁶A. Sukhov, P. P. Horley, C. L. Jia, and J. Berakdar, *J. Appl. Phys.* **113**, 013908 (2013).
- ⁷I. Fina, N. Dix, J. M. Rebled, P. Gemeiner, X. Marti, F. Peiro, B. Dkhil, F. Sanchez, L. Fabrega, and J. Fontcuberta, *Nanoscale* **5**, 8037 (2013).
- ⁸N. Jedrecy, H. J. von Bardeleben, V. Badjcek, D. Demaille, D. Stanesco, H. Magnan, and A. Barbier, *Phys. Rev. B* **88**, 121409 (2013).
- ⁹W. Erenstein, N. D. Mathur, and J. F. Scott, *Nature* **442**, 759 (2006).
- ¹⁰P. Curie, *J. Phys.* 3e, se'rie t.III, 393 (1894); reprinted 1908 in *Oeuvres de Pierre Curie* (Gauthier-Villars, Paris), pp. 136–137.
- ¹¹D. N. Astrof, *Sov. Phys. JETP* **11**, 708 (1960).
- ¹²C. W. Nan, *Phys. Rev. B* **50**, 6082 (1994).
- ¹³F. Xue, J. Hu, S. X. Wang, and J. L. He, *Appl. Phys. Lett.* **106**, 262902 (2015).
- ¹⁴H. Zheng, J. Wang, S. E. Lofland, Z. Ma, L. Mohaddes-Ardabili, T. Zhao, L. Salamanca-Riba, S. R. Shinde, S. B. Ogale, F. Bai, D. Viehland, Y. Jia, D. G. Schlom, M. Wuttig, A. Roytburd, and R. Ramesh, *Science* **303**, 661 (2004).
- ¹⁵G. Liu, C. W. Nan, Z. K. Xu, and H. Chen, *J. Phys. D: Appl. Phys.* **38**, 2321 (2005).
- ¹⁶C. L. Jia, T. L. Wei, C. J. Jiang, D. S. Xue, A. Sukhov, and J. Berakdar, *Phys. Rev. B* **90**, 054423 (2014).
- ¹⁷Z. D. Wang and M. J. Grimson, “Driving skyrmions on a composite multiferroic lattice,” e-print [arXiv:1601.01383](https://arxiv.org/abs/1601.01383).
- ¹⁸R. F. L. Evans, U. Atxitia, and R. W. Chantrell, *Phys. Rev. B* **91**, 144425 (2015).
- ¹⁹H. B. Jang and M. J. Grimson, *Phys. Rev. B* **55**, 12556 (1997).
- ²⁰R. Blinc and B. Zeks, *Soft Modes Ferroelectrics and Antiferroelectrics* (North-Holland Pub. Co., North Holland, Amsterdam, 1974).
- ²¹P. G. de Gennes, *Solid State Commun.* **1**, 132 (1963).
- ²²R. J. Elliott and A. P. Young, *Ferroelectrics* **7**, 23 (1974).
- ²³R. Pirc and R. Blinc, *Phys. Rev. B* **70**, 134107 (2004).
- ²⁴Z. D. Wang and M. J. Grimson, “Pseudo-spin based dynamical model for polarization switching in ferroelectrics,” e-print [arXiv:1506.8500](https://arxiv.org/abs/1506.8500).
- ²⁵M. Thesberg and E. S. Sørensen, *Phys. Rev. B* **90**, 115117 (2014).
- ²⁶Y. L. Li, K. Xu, S. Y. Hu, J. Suter, D. K. Schreiber, P. Ramuhalli, B. R. Johnson, and J. McCloy, *J. Phys. D: Appl. Phys.* **48**, 305001 (2015).
- ²⁷M. Lakshmanan, *Philos. Trans. R. Soc., A* **369**, 1280 (2011).
- ²⁸See supplementary material at <http://dx.doi.org/10.1063/1.4944604> for animations of the magnetic spin, the electric pseudospin, and the magnetic domain wall motion in Fig. 3.
- ²⁹H. B. Jang and M. J. Grimson, *J. Phys.: Condens. Matter* **11**, 5045 (1999).
- ³⁰P. Pfeuty, *Ann. Phys.* **57**, 79 (1970).
- ³¹C. Kittel, *Introduction to Solid State Physics*, 8th ed. (John Wiley & Sons, 2005), Chap. 16.
- ³²C. Aron, D. G. Barci, L. F. Cugliandolo, Z. Gonzalez, and G. S. Lozano, *J. Stat. Mech.: Theory Exp.* **2014**, P09008.
- ³³L. Chotorlishvili, S. R. Etesami, J. Berakdar, R. Khomeriki, and J. Ren, *Phys. Rev. B* **92**, 134424 (2015).